sustainability

Article

Filtering Power Divider Design Using Resonant LC Branches for 5G Low-Band Applications

Saeed Roshani [1,*], Salah I. Yahya [2,3], Ban M. Alameri [4], Yaqeen Sabah Mezaal [5], Louis W. Y. Liu [6] and Sobhan Roshani [1]

1 Department of Electrical Engineering, Kermanshah Branch, Islamic Azad University, Kermanshah, Iran
2 Department of Communication and Computer Engineering, Cihan University-Erbil, Erbil 44001, Iraq
3 Department of Software Engineering, Faculty of Engineering, Koya University, Koya KOY45, Iraq
4 Department of Electrical Engineering, Faculty of Engineering, Mustansiriyah University, Baghdad 10053, Iraq
5 Medical Instrumentation Engineering Department, Al-Esraa University College, Baghdad 10071, Iraq
6 Faculty of Engineering, Vietnamese-German University, Binh Duong New City 75000, Binh Duong, Vietnam
* Correspondence: s_roshany@yahoo.com

Abstract: This paper proposes an ultra-compact filtering power divider with a wide harmonic suppression band. In this design, the proposed power divider (PD) in the ideal case has 100% size reduction and an infinite number of harmonics suppression. However, in the real case, the proposed divider has a 92% size reduction and suppresses the 2nd to 45th harmonics. The small-proposed divider is designed at 0.9 GHz. The typical Wilkinson divider has two long quarter-wavelength branches. In the proposed design, new resonant series LC branches are used instead of the divider's typical branches, leading to performance improvements in the proposed PD. To the best of the authors' knowledge, the proposed filtering PD has the best size reduction, and harmonics suppression reported thus far. The proposed divider has a filtering response with good insertion loss at the passband, which is desirable for modern communication systems.

Keywords: compact power divider; lumped components; performance improvement; size reduction

check for updates

Citation: Roshani, S.; Yahya, S.I.; Alameri, B.M.; Mezaal, Y.S.; Liu, L.W.Y.; Roshani, S. Filtering Power Divider Design Using Resonant LC Branches for 5G Low-Band Applications. *Sustainability* **2022**, *14*, 12291. https://doi.org/10.3390/su141912291

Academic Editors: Vanlin Sathya, Madhuri Siddula and Kalpana Naidu

Received: 2 September 2022
Accepted: 26 September 2022
Published: 27 September 2022

Publisher's Note: MDPI stays neutral with regard to jurisdictional claims in published maps and institutional affiliations.

Copyright: © 2022 by the authors. Licensee MDPI, Basel, Switzerland. This article is an open access article distributed under the terms and conditions of the Creative Commons Attribution (CC BY) license (https://creativecommons.org/licenses/by/4.0/).

1. Introduction

Power dividers (PDs) are essential devices commonly used in communication circuits. PDs are used for power division or combination in amplifiers, antennas, phase shifters, mixers, modulators, and frequency multipliers [1]. Dividers have been widely used in modern 5G communications circuits and systems— the specifications of sub-6 GHz, 5G applications are explained in [2,3]. In addition, the dividers can be integrated into the MIMO antenna applications [4,5].

Two common types of PDs in microwave applications are Wilkinson and Gysel. A typical Wilkinson power divider (WPD) has two long quarter-wave ($\lambda/4$) length branches with a 100 Ω lumped resistor between output ports. A Gysel power divider has six $\lambda/4$ length branches, and two 50 Ω lumped resistors. Both of these dividers are large (especially Gysel) and have undesirable harmonics. Several works have partially made improvements on these drawbacks in recent decades. Open-ended stubs were exploited to address the large size and undesirable harmonics in [1]. However, this method is simple: many open-ended stubs are needed to remove many harmonics, and each applied stub creates one narrow transmission zero, which helps the suppression band.

In some designs, the electronic band gap (EBG) cells [6,7] and defected ground structure (DGS) [8,9] are used to overcome these drawbacks of the standard dividers. An additional stage is needed for these two structures in the fabrication process, which results in the complexity of circuit design. Resonator cells [10–14] are widely used in the divider branches to create filtering responses, remove harmonics and reduce the length of the long branches. The applied resonators increase the insertion losses of the dividers, and all these mentioned power dividers suffer from high insertion losses.

In some research [15,16], coupled lines were used in the divider structure to suppress unwanted harmonics. With the applied coupled lines method, only signals at operating frequency were passed, and the signals at other frequencies were eliminated, which creates filtering responses. Unfortunately, the coupled lines method cannot improve the size of the circuit. For example, the size of both dividers in [15,16] is more significant than the typical divider. Recently higher frequencies for power dividers have been achieved using optical fiber substrates [17,18]. In addition, methods of optimization and artificial intelligence (AI) have been recently used to design power dividers and other microwave components [19,20].

Resonators are also used for performance improvement in the power dividers [21–26]. Different shapes of the resonators have been recently presented, such as U-shaped [21], T-shaped [22], Pi-shaped, [23] stepped impedance [24], and patch resonators [25,26]. In [25], patch resonators were used to design a filtering power divider. The circular divider was designed in [25], and a dual-band operation was achieved. However, the obtained suppression band was not wide enough, and the undesirable harmonics can pass through the divider. Patch resonators and meandered lines were used in [26] to design a radial filtering divider. An acceptable suppression band was obtained in [26], but the final size of the divider was larger than the typical structure. Moreover, artificial intelligence (AI) techniques [27–31] and optimization methods [32–38], which are useful tools, have been recently applied to design PDs and other microwave components [39,40].

All the discussed works in the literature have partially improved the large size and harmonic presence drawbacks of the typical power divider. However, the proposed work has solved these two drawbacks with the best results compared to the previous works, such that to the author's best knowledge, the best size reduction and harmonic suppression are achieved simultaneously. This paper incorporates the LC lumped elements into proposed developed LC branches, which can be used instead of the power divider main branches. The proposed new branches have resulted in a compact design of the power divider with the desired percentage of miniaturization. In addition, a filtering response with a wide suppression band has been obtained for the proposed divider using the developed LC branches.

2. Structure of the Typical WPD

As depicted in Figure 1, the typical Wilkinson divider has two long $\lambda/4$ branches and a lumped 100 ohms resistor. The microstrip realization of the normal WPD is shown in Figure 2. This structure has a large size of $\lambda/8 \times \lambda/8$. This large size is the first drawback of this typical divider.

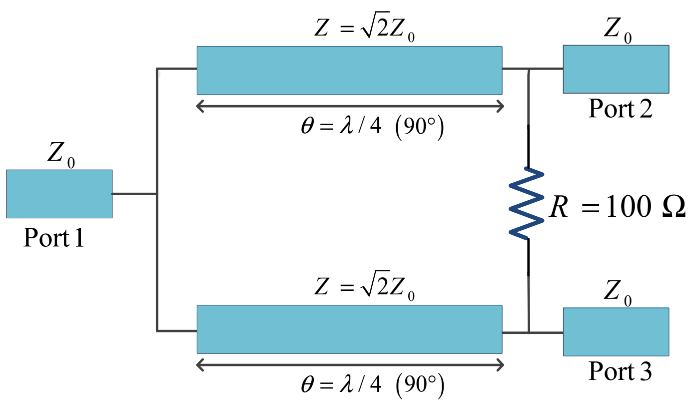

Figure 1. Schematic of a typical WPD.

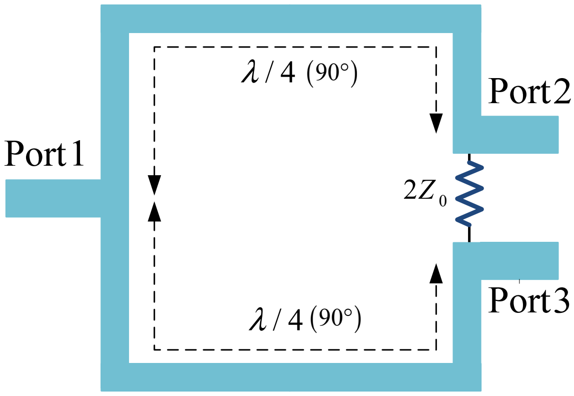

Figure 2. Microstrip realization of the typical WPD.

An Agilent ADS simulator carried out the divider design, and the circuit simulator and electromagnetic (EM) simulator were carried out based on the Duroid5880 substrate with $\varepsilon_r = 2.2$ and 0.508 mm thickness.

The typical WPD frequency response is depicted in Figure 3. The typical divider performs well at the operating frequency. Nonetheless, this structure passes unwanted signals at higher frequencies, like the desired signals at operating frequencies, without suppression.

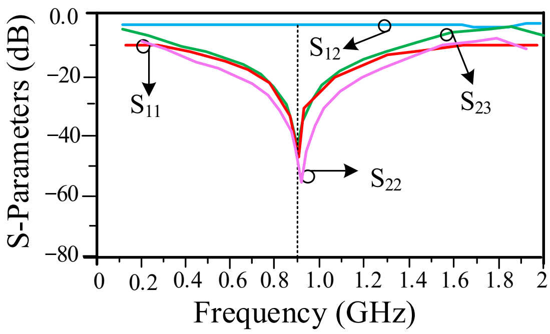

Figure 3. Frequency response of the typical WPD.

3. Proposed WPD Structure

As mentioned in the previous section, the typical divider not only has a large size but also suffers from undesirable harmonics. To overcome these drawbacks proposed LC branch is designed to provide a suppression band and miniaturize the circuit size. The proposed LC branch's structure is shown in Figure 4. The developed LC branch has a very short length and provides a filtering response at the desired frequency.

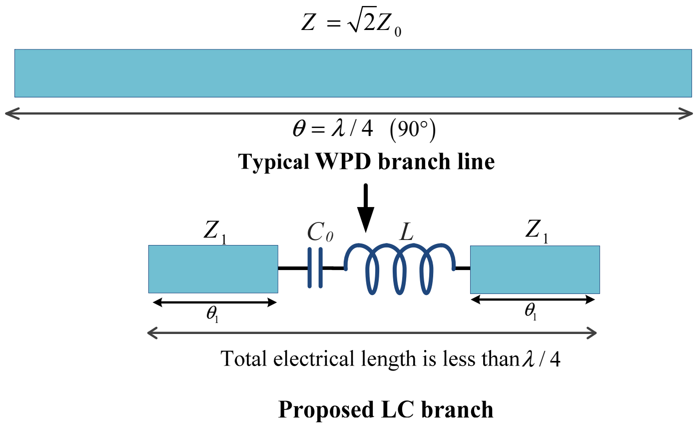

Figure 4. Structure of the typical and proposed developed branches.

4. Proposed LC Branch Analysis

The typical and proposed branches should have the same response at the operating frequency. Thus, the ABCD matrix of these branches should be equal. The main λ/4 branch line has one microstrip line, and the ABCD matrix for this part is demonstrated with M_{MB}. The proposed branch line has two microstrip lines with an electrical length of θ_1 and a series of lumped components. The ABCD matrix for the first part is noted with M_1, and the ABCD matrix for the series lumped elements is noted with M_{LMP}.

As mentioned, the ABCD matrices of the proposed LC branch and normal branch should be equal; therefore, the equation is written in (1):

$$M_1 \times M_{LMP} \times M_1 = M_{MB} \tag{1}$$

The values of M_1, M_{LMP}, and M_{MB} are written in Equations (2)–(4):

$$M_{QWL} = \begin{bmatrix} 0 & j\sqrt{2}Z_0 \\ j/\sqrt{2}Z_0 & 0 \end{bmatrix} \tag{2}$$

$$M_1 = \begin{bmatrix} \cos(\theta_1) & jZ_1 \sin(\theta_1) \\ jY_1 \sin(\theta_1) & \cos(\theta_1) \end{bmatrix} \tag{3}$$

$$M_{LMP} = \begin{bmatrix} 1 & jL\omega - j/(C_0\omega) \\ 0 & 1 \end{bmatrix} \tag{4}$$

The applied inductor in the proposed branch consists of two series inductors of L_0 and L_m. The L_m with two adjacent transmission lines creates a composite line, which provides a miniaturization of the power divider. The L_0C_0 is tuned at the central frequency (f_0), as illustrated in Figure 5. Therefore, the M_{LMP} matrix can be written in the analysis at the central frequency as (5).

$$M_{LC} = \begin{bmatrix} 1 & jL_m\omega \\ 0 & 1 \end{bmatrix} \tag{5}$$

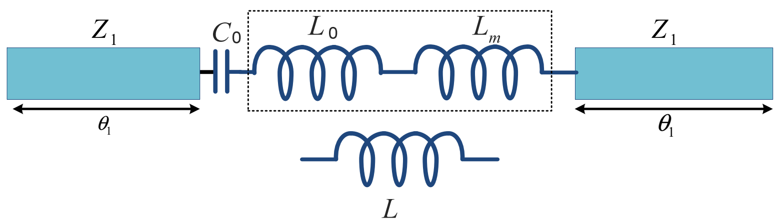

Figure 5. Internal inductors of the proposed developed branch.

By solving Equation (1) and substituting Equations (1)–(5), Equations (6)–(9) can be written:

$$2Z_1 = L_m\omega_0 \tan(2\theta_1) \tag{6}$$

$$\sqrt{2} = \frac{Z_1}{Z_0}\sin(2\theta_1) + \frac{L_m\omega_0}{2Z_0} + \frac{L_m\omega_0}{2Z_0}\cos(2\theta_1) \tag{7}$$

$$\frac{1}{\sqrt{2}} = \frac{Z_0}{Z_1}\sin(2\theta_1) - \frac{Z_0L_m\omega_0}{2{Z_1}^2} + \frac{Z_0L_m\omega_0}{2{Z_1}^2}\cos(2\theta_1) \tag{8}$$

From Equations (7) and (8), Equation (9) is achieved as follows:

$$2 - \frac{{Z_1}^2}{{Z_0}^2} = \frac{\sqrt{2}L_m\omega_0}{Z_0} \tag{9}$$

By solving Equation (9), the normalized value of Z_1 can be calculated as written in (10):

$$\frac{Z_1}{Z_0} = \frac{-\sqrt{2} + \sqrt{2 + \tan(2\theta_1)^2}}{\tan(2\theta_1)} \tag{10}$$

5. Proposed WPD with LC Branch Analysis

The proposed structure of the WPD with the presented LC branches is shown in Figure 6. The design goal is a 900 MHz divider with a 90% size reduction.

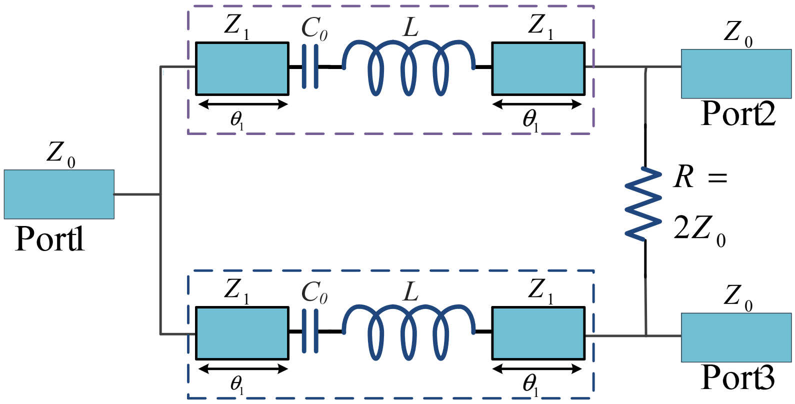

Figure 6. Structure of the proposed WPD with the series LC branches.

The occupied size of the typical WPD is λ/8 × λ/8. In the proposed WPD, to have a 90% size reduction, the occupied size should be 0.1 × (λ/8 × λ/8). Therefore, the proposed branch length (θ_1 + length of lumped components + θ_1) should be 30°, which is equal to 0.08 λ. Thus, the θ_1 should be approximately 15° (0.04 λ). The lengths of the lumped components (L and C) are neglected. Until now, the value of the θ_1 has been calculated, and to calculate the unknown parameter of Z_1, from (10) and considering Z_0 = 50 Ω, the Z_1 can be determined as follows:

$$\frac{Z_1}{Z_0} = \frac{-\sqrt{2} + \sqrt{2 + \tan(30)^2}}{\tan(30)} \tag{11}$$

The value of impedance is equal to Z_1 = 18.9 Ω. The dimensions of the proposed branches with the applied substrate of Duroid5880 substrate with ε_r = 2.2 and 0.508 mm thickness are depicted in Figure 7.

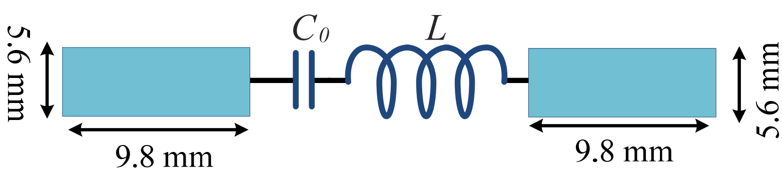

Figure 7. The dimensions of the proposed branches with the applied substrate.

As seen in Figure 5, the applied inductor consists of two series inductors of L_0 and L_m. The value of L_m can be easily obtained from Equation (6), considering the 900 MHz operating frequency as follows:

$$L_m = \frac{2Z_1}{w \times \tan(30)} \tag{12}$$

with Z_1 = 18.9 Ω and w = 2π × (900 MHz), the value of L_m is 11.58 nH. L_0 and C_0 can be obtained from (13), which have several answers. If we select 0.5 PF for the applied capacitor according to (13), the L_0 value is 62 nH:

$$w = \frac{1}{\sqrt{L_0 \times C}} \tag{13}$$

The value of the applied inductor can be calculated from (14), which is equal to 73.5 nH:

$$\mathrm{L} = L_0 + L_m \tag{14}$$

6. The Proposed Power Divider Design

The design process of the proposed divider is depicted in Figure 8. At first, a typical WPD at 900 MHz, with a large size, is designed. The first design of WPD is proposed according to the analysis, which has an 82% size reduction. The length of the proposed transmission line is obtained analytically. Finally, the optimized WPD is presented and fabricated with a 92% size reduction.

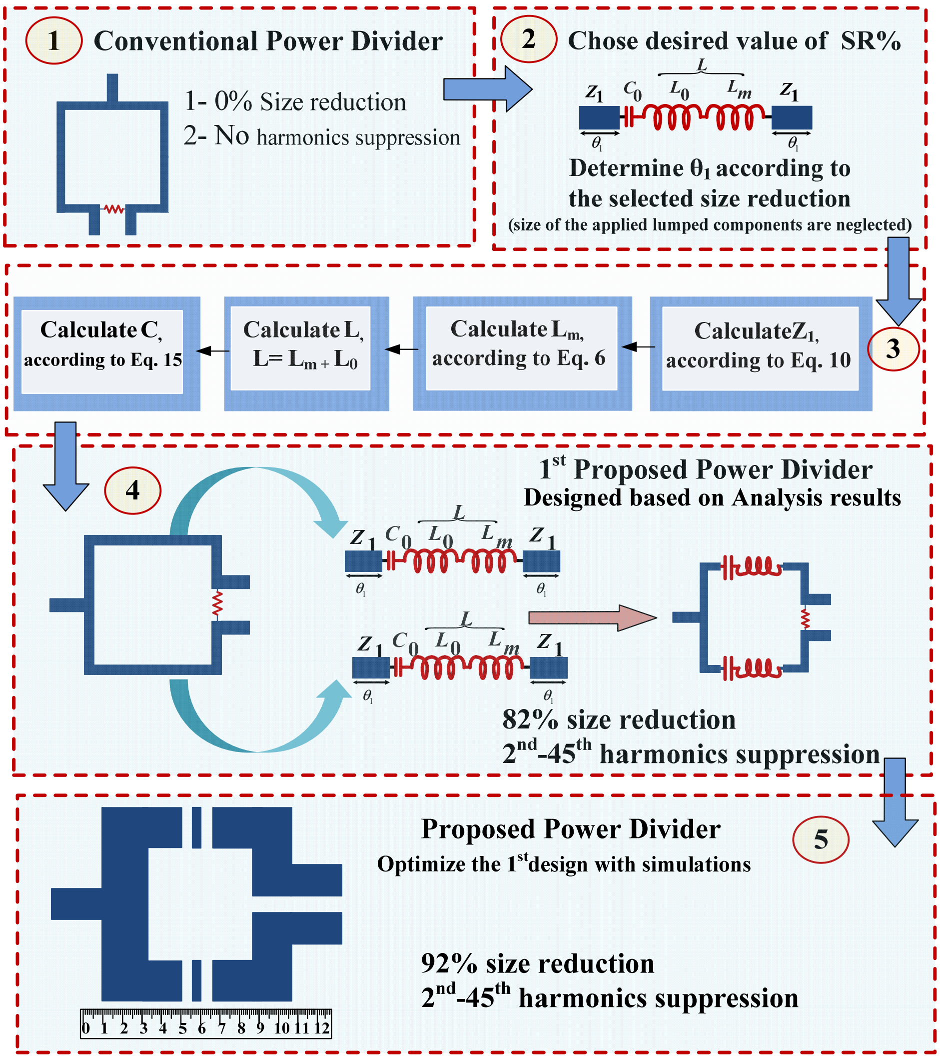

Figure 8. The design process of the proposed divider.

6.1. Typical WPD Design

In this section, the typical WPD at 900 MHz is realized with microstrip lines to have better compression at first. The realized typical WPD is shown in Figure 9a. The typical

WPD has a size of 33.9 mm × 34.7 mm. The scattering parameters of typical WPD are depicted in Figure 9b, showing the divider's correct performance at 900 MHz.

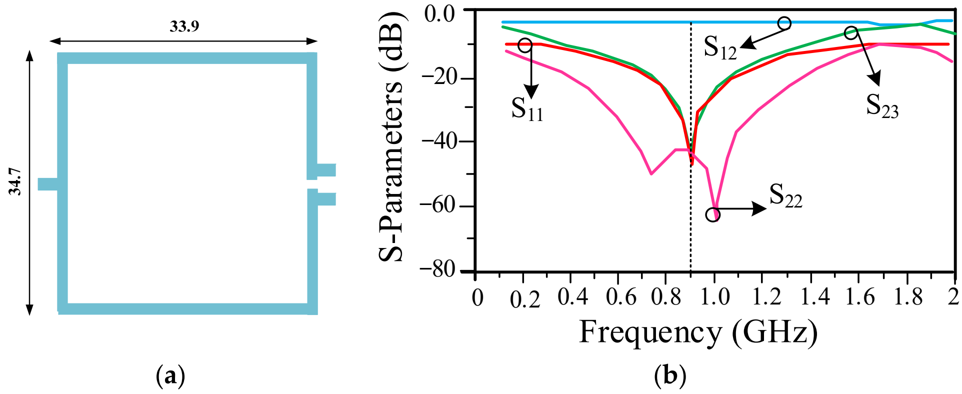

Figure 9. Typical WPD at 900 MHz with the applied substrate. (**a**) Layout and (**b**) S-parameters.

6.2. First Design of the Proposed WPD without Optimization

In the second step, two proposed developed LC branch lines, designed in Section 5 with calculated dimensions, are used instead of the long branches of the typical divider. The proposed WPD is depicted in Figure 10. The overall size of the proposed WPD is 13.9 mm × 15.3 mm, which offers an 82% reduction in size compared to typical WPD. In the simulation process, some values are tuned to have better results. The obtained values from analysis, simulation and measurement are listed in Table 1.

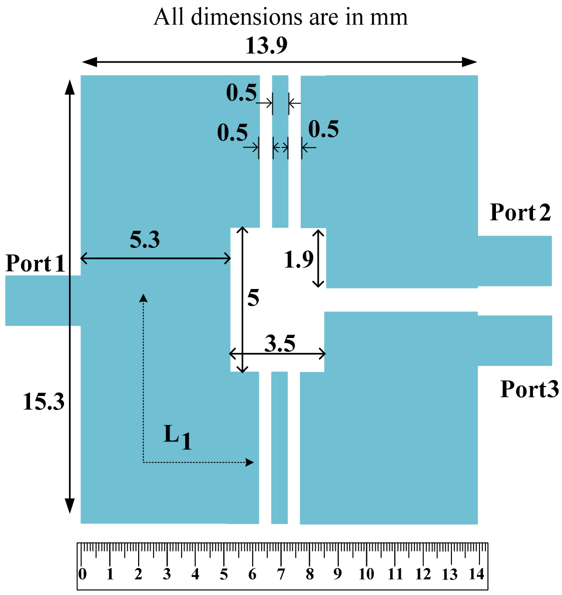

Figure 10. The first design of the proposed WPD at 900 MHz 82% size reduction.

The first design of the proposed WPD response at the main frequency is shown in Figure 11a. These parameters at a wide frequency range are depicted in Figure 11b. This divider performs correctly at 900 MHz and suppresses the 2nd to 45th unwanted harmonics with a high level of attenuation.

Table 1. Obtained values from the simulation and measurement.

Values	Analysis	1st Design	2nd Design	Fabrication
W (mm)	5.6	5.3	3.2	3.2
L_1 (mm)	9.8	9.4	6.5	6.5
L (nH)	73.5	66	68.3	68
C (pF)	0.5	0.43	0.43	0.43
f (MHz)	900	900	900	900
Size Reduction	90%	82%	92%	92%
Harmonics Suppression	∞	2nd–45th	2nd–45th	2nd–45th

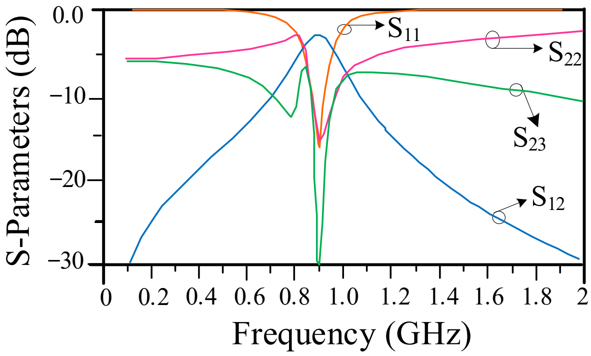

(**a**)

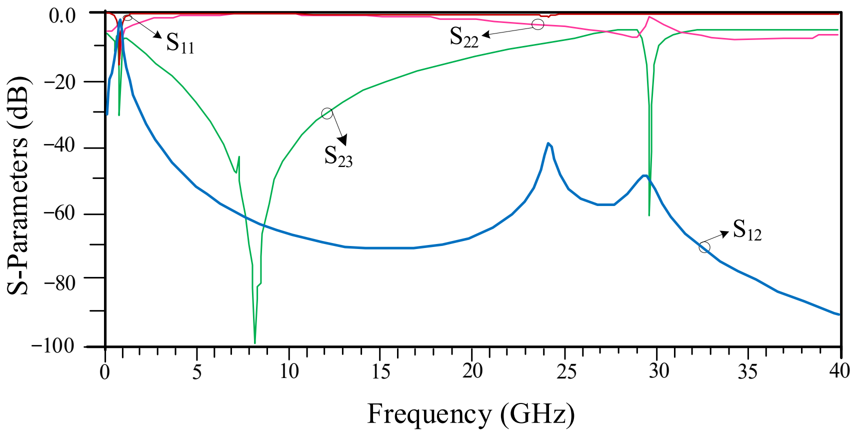

(**b**)

Figure 11. The scattering parameters at (**a**) operating band and (**b**) wide frequency range for the first design of the proposed WPD with 82% size reduction.

6.3. Second Design of the Proposed WPD with Improvement

In the final step, the proposed WPD is presented, and the layout of the proposed divider is depicted in Figure 12. The proposed WPD final size is only 9.9 mm ×10.4 mm, which shows a 92% size miniaturization.

The scattering parameters of the proposed WPD near the orating frequency are shown in Figure 13a. The proposed WPD acts correctly at 900 MHz. The S_{21} parameter at the operating frequency is −3.3 dB, which offers about 0.3 dB insertion loss. The S_{11}, S_{22}, and S_{23} parameters are about −20 dB, which shows good divider performance at the operating frequency. The proposed WPD has noticeable performance at higher frequencies. A wide stopband has been obtained for the proposed divider from 1.8 GHz up to 40 GHz, which shows excellent harmonics suppression. The simulated results of the proposed WPD are depicted in Figure 13b.

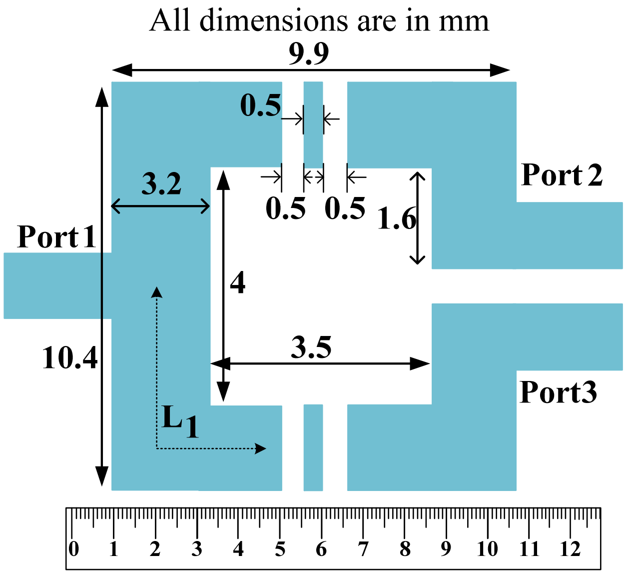

Figure 12. The proposed WPD at 900 MHz with a 92% size reduction.

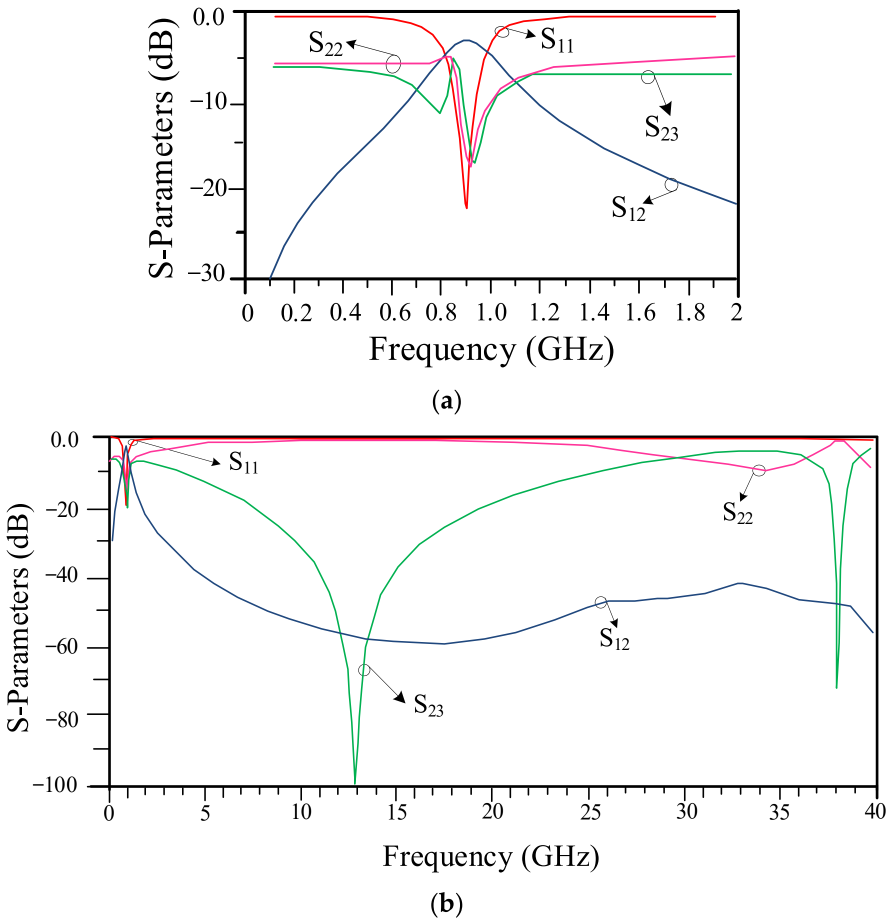

Figure 13. The scattering parameters at (**a**) operating band and (**b**) wide frequency range of the proposed WPD with 92% size reduction.

The layout comparison between the proposed and typical WPD is depicted in Figure 14. The proposed WPD only occupies 0.08% of the normal WPD, showing a 92% size reduction. The fabricated photo of the proposed WPD is depicted in Figure 15.

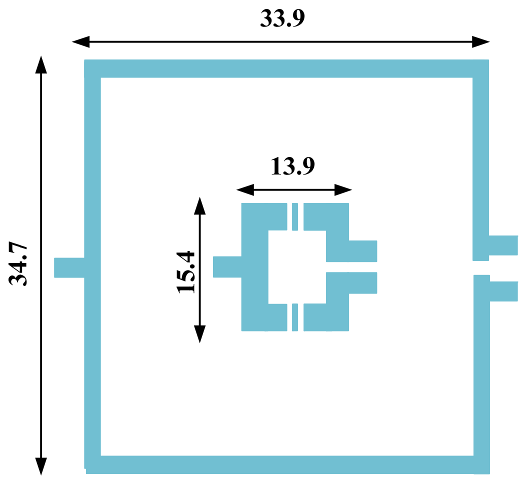

Figure 14. The layout comparison between proposed and typical WPD at 900 MHZ.

Figure 15. Fabricated photo of the proposed 900 MHz divider with a 92% size reduction.

The proposed divider's fabrication accuracy is critical due to the narrow microstrip lines applied. Any fabrication error or substrate loss will disturb frequency response. Therefore, the photolithography method is used to create an accurate prototype, and after this step, the lumped capacitors and inductors are soldered on the prototype.

The simulated and measured results of the fabricated divider are shown in Figure 16. The proposed divider frequency response is depicted in Figure 16a, and a wide operating frequency range is illustrated in Figure 16b.

The performances of the designed WPD and related works are compared in Table 2. The proposed WPD has the most compact size and best suppression band among the reported studies. The size reduction in Table 2 is calculated based on the normalized size of the dividers.

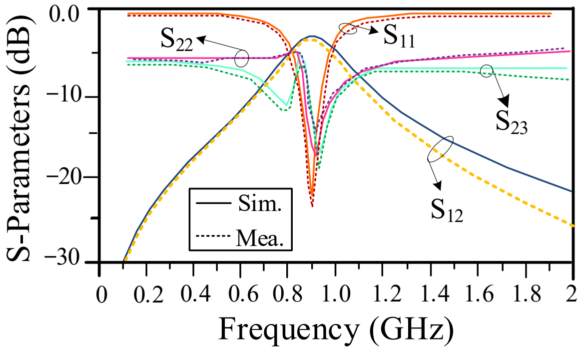

(**a**)

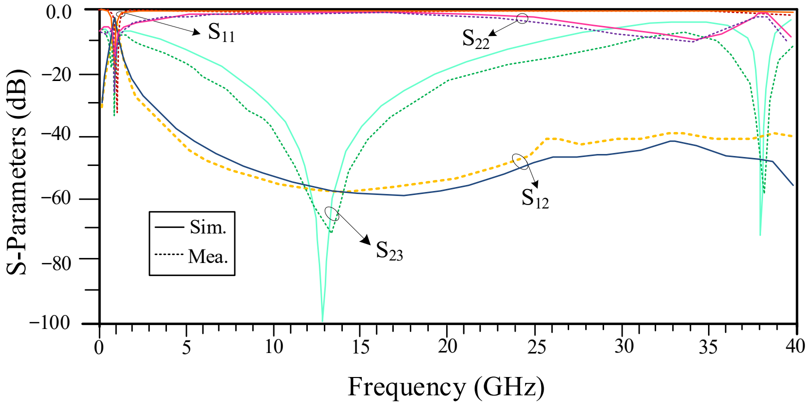

(**b**)

Figure 16. The simulation and measurement frequency response of the proposed WPD (**a**) at operating frequency (**b**) in the wide frequency range.

Table 2. Performance summary of the proposed WPD and related works.

Ref	Freq (GHz)	Size Reduction	Number of Harmonics Suppression	Methods
[41]	1	0%	2nd–4th	Open stubs
[42]	2.4	70%	2nd–5th	EBG Cells
[43]	1.5	0%	2nd–3rd	DGS Cells
[44]	2.4	39%	2nd-3rd	EBG Cells
[45]	0.9	66%	2nd–3rd	Coupled Line
[46]	1.5	0%	2nd–3rd	Lumped Capacitor
[47]	2.4	44%	2nd–3rd	Resonator Cell
[48]	0.9	47%	3rd	Resonator Cell
[49]	1	55%	2nd–5th	Open Stubs
[50]	2.65	63%	3rd and 5th	Open Stubs
[51]	1	54%	2nd–7th	Open Stubs
[52]	1	71%	2nd–12th	Resonator Cell & Open Stubs
[53]	1	0%	2nd–3rd	Open Stubs
[54]	1	0%	2nd	Open And Short Stubs
[55]	2	0%	2nd	Resonator Cell & Open Stubs
[56]	1.9	55 %	2nd–4th	Resonator Cell
[57]	1.5	52%	3rd–6th	Lumped Element & Resonator Cell
[58]	2.4	0%	2nd–3rd	Resonator Cell
[59]	1.5	16%	3rd–4th	Lumped Capacitor
[60]	1	60%	2nd–4th	Lumped Inductor
[61]	1.65	35%	3rd and 5th	Open Stubs
[62]	0.9	0%	2nd–4th	Open And Short Stubs
[63]	2	50%	2nd–14th	Resonator Cell
[64]	0.7	73%	2nd–15th	Aperiodic Open Stubs
[65]	0.8	82.8%	2nd–25th	LC Branches
This Work	0.9	92%	2nd–45th	LC Branches

7. Conclusions

A 900 MHz WPD, with excellent size reduction and harmonics suppression, is designed, analyzed, and implemented in this paper. In this WPD, compact proposed series LC branches are used instead of the long microstrip lines in the typical WPD, which leads to excellent compact size, filtering response, and performance improvement. The designed WPD has a 92% size reduction compared to the typical WPD and suppresses the 2nd to 45th unwanted harmonics. The proposed WPD has the most compact size and best suppression band, which have been reported up until now. In this paper, the WPD is initially designed analytically, then simulated with ADS software, and the proposed device is fabricated at the end. All of the calculated, simulation and measured values have good agreements, confirming the proposed design's validity.

Author Contributions: Conceptualization, S.R. (Saeed Roshani) and S.R. (Sobhan Roshani); Formal analysis, B.M.A. and L.W.Y.L.; Methodology, S.I.Y. and Y.S.M.; Software, B.M.A., Y.S.M., L.W.Y.L. and S.R. (Sobhan Roshani); Validation, Y.S.M.; Writing—original draft, S.R. (Saeed Roshani) and S.R. (Sobhan Roshani); Writing—review & editing, S.I.Y. All authors have read and agreed to the published version of the manuscript.

Funding: The authors would like to thank the Kermanshah Branch, Islamic Azad University, for the financial support of this research project.

Data Availability Statement: All the material conducted in the study is mentioned in the article.

Acknowledgments: The authors would like to thank the Kermanshah Branch, Islamic Azad University, for the financial support of this research project.

Conflicts of Interest: The authors declare no conflict of interest.

References

1. Roshani, S.; Roshani, S.; Zarinitabar, A. A modified Wilkinson power divider with ultra harmonic suppression using open stubs and lowpass filters. *Analog Integr. Circuits Signal Process.* **2019**, *98*, 395–399. [CrossRef]
2. Radanliev, P.; de Roure, D. Review of Algorithms for Artificial Intelligence on Low Memory Devices. *IEEE Access* **2021**, *9*, 109986–109993. [CrossRef]
3. Radanliev, P.; De Roure, D.; Walton, R.; Van Kleek, M.; Montalvo, R.M.; Santos, O.; Maddox, L.; Cannady, S. COVID-19 what have we learned? The rise of social machines and connected devices in pandemic management following the concepts of predictive, preventive and personalized medicine. *EPMA J.* **2020**, *11*, 311–332. [CrossRef] [PubMed]
4. Alharbi, A.G.; Kulkarni, J.; Desai, A.; Sim, C.-Y.; Poddar, A. A Multi-Slot Two-Antenna MIMO with High Isolation for Sub-6 GHz 5G/IEEE802.11ac/ax/C-Band/X-Band Wireless and Satellite Applications. *Electronics* **2022**, *11*, 473. [CrossRef]
5. Kulkarni, J.; Alharbi, A.G.; Desai, A.; Sim, C.-Y.; Poddar, A. Design and Analysis of Wideband Flexible Self-Isolating MIMO Antennas for Sub-6 GHz 5G and WLAN Smartphone Terminals. *Electronics* **2021**, *10*, 3031. [CrossRef]
6. Ko, Y.J.; Park, J.Y.; Bu, J.U. Fully integrated unequal Wilkinson power divider with EBG CPW. *IEEE Microw. Wirel. Compon. Lett.* **2003**, *22*, 276–278.
7. Ooi, B.L. Compact EBG in-phase hybrid-ring equal power divider. *IEEE Trans. Microw. Theory Tech.* **2005**, *53*, 2329–2334.
8. Gupta, N.; Ghosh, P.; Toppo, M. A miniaturized Wilkinson power divider using DGS and fractal structure for GSM application. *Prog. Electromagn. Res. Lett.* **2011**, *27*, 25–31. [CrossRef]
9. Kazerooni, M.; Fartookzadeh, M. Design of a Two Octave Gysel power divider using DGS and DMS. *J. Commun. Eng.* **2013**, *2*, 73–88.
10. Song, K.; Ren, X.; Chen, F.; Fan, Y. Compact in-phase power divider integrated filtering response using spiral resonator. *IET Microw. Antennas Propag.* **2013**, *8*, 228–234. [CrossRef]
11. Liu, H.; Liu, C.; Dai, X.; He, S. Design of novel compact dual-band filtering power divider using stepped-impedance resonators with high selectivity. *Int. J. RF Microw. Comput. Eng.* **2016**, *26*, 262–267. [CrossRef]
12. Li, X.; Shao, Z.; Shen, M.; He, Z. High selectivity tunable filtering power divider based on liquid crystal technology for microwave applications. *J. Electromagn. Waves Appl.* **2016**, *30*, 825–833. [CrossRef]
13. Moloudian, G.; Lalbakhsh, A.; Bahrami, S. A Harmonic-Free Wilkinson Power Divider Using Lowpass Resonators. In Proceedings of the 2022 16th European Conference on Antennas and Propagation (EuCAP), Madrid, Spain, 27 March 2022; pp. 1–4.
14. Lalbakhsh, A.; Ghaderi, A.; Mohyuddin, W.; Simorangkir, R.B.; Bayat-Makou, N.; Ahmad, M.S.; Lee, G.H.; Kim, K.W. A compact C-band bandpass filter with an adjustable dual-band suitable for satellite communication systems. *Electronics* **2020**, *9*, 1088. [CrossRef]
15. Wang, Y.; Zhang, X.Y.; Liu, F.X.; Lee, J.C. A compact bandpass Wilkinson power divider with ultra-wideband harmonic suppression. *IEEE Microw. Wireless Compon. Lett.* **2017**, *27*, 888–890. [CrossRef]

16. Chen, M.T.; Tang, C.W. Design of the filtering power divider with a wide passband and stopband. *IEEE Microw. Wireless Compon. Lett.* **2018**, *28*, 570–572. [CrossRef]
17. Parandin, F.; Olyaee, S.; Kamarian, R.; Jomour, M. Design and Simulation of Linear All-Optical Comparator Based on Square-Lattice Photonic Crystals. *Photonics* **2022**, *9*, 459. [CrossRef]
18. Parandin, F.; Sheykhian, A. Design and simulation of a 2 × 1 All-Optical multiplexer based on photonic crystals. *Opt. Laser Technol.* **2022**, *151*, 108021. [CrossRef]
19. Roshani, M.; Sattari, M.A.; Ali, P.J.M.; Roshani, G.H.; Nazemi, B.; Corniani, E.; Nazemi, E. Application of GMDH neural network technique to improve measuring precision of a simplified photon attenuation based two-phase flowmeter. *Flow Meas. Instrum.* **2020**, *75*, 101804. [CrossRef]
20. Nazemi, E.; Roshani, G.H.; Feghhi, S.A.; Setayeshi, S.; Zadeh, E.E.; Fatehi, A. Optimization of a method for identifying the flow regime and measuring void fraction in a broad beam gamma-ray attenuation technique. *Int. J. Hydrog. Energy* **2016**, *41*, 7438–7444. [CrossRef]
21. Karimi, G.; Lalbakhsh, A.; Dehghani, K.; Siahkamari, H. Analysis of Novel Approach to Design of Ultra-wide Stopband Microstrip Low-Pass Filter Using Modified U-Shaped Resonator. *ETRI J.* **2015**, *37*, 945–950. [CrossRef]
22. Sariri, H.; Rahmani, Z.; Lalbakhsh, A.; Majidifar, S. Compact LPF Using T-shaped Resonator. *Frequenz* **2013**, *67*, 17–20. [CrossRef]
23. Wang, Z.; Park, C.W. Multiband pi-shaped structure with resonators for tri-band Wilkinson power divider and tri-band rat-race coupler. In Proceedings of the 2012 IEEE/MTT-S International Microwave Symposium Digest, Montreal, QC, Canada, 17–22 June 2012; IEEE: Piscataway Township, NJ, USA; pp. 1–3.
24. Dehghani, K.; Karimi, G.; Lalbakhsh, A.; Maki, S. Design of lowpass filter using novel stepped impedance resonator. *Electron. Lett.* **2014**, *50*, 37–39. [CrossRef]
25. Zhang, Q.; Zhang, G.; Liu, Z.; Chen, W.; Tang, W. Dual-Band Filtering Power Divider Based on a Single Circular Patch Resonator with Improved Bandwidths and Good Isolation. *IEEE Trans. Circuits Syst. II Express Briefs* **2021**, *68*, 3411–3415. [CrossRef]
26. Chen, S.; Qi, S.; Chen, X.; Sun, G.; Wu, W. Five-way radial filtering power divider using back-to-back quarter-mode substrate-integrated waveguide and microstrip resonator. *Electron. Lett.* **2021**, *57*, 888–890. [CrossRef]
27. Roshani, G.; Hanus, R.; Khazaei, A.; Zych, M.; Nazemi, E.; Mosorov, V. Densityand velocity determination for single-phase flow based on radiotracertechnique and neuralnetworks. *Flow Meas. Instrum.* **2018**, *61*, 9–14. [CrossRef]
28. Hashemi, A.; Dowlatshahi, M.B.; Nezamabadi-Pour, H. Ensemble of feature selection algorithms: A multi-criteria decision-making approach. *Int. J. Mach. Learn. Cybern.* **2021**, *13*, 49–69. [CrossRef]
29. Sattari, M.A.; Roshani, G.H.; Hanus, R.; Nazemi, E. Applicability of time-domain feature extractionmethods and artificial intelligence in two-phaseflow meters based on gamma-ray absorption technique. *Measurement* **2021**, *168*, 108474. [CrossRef]
30. Beiranvand, F.; Mehrdad, V.; Dowlatshahi, M.B. Unsupervised feature selection for image classification: A bipartite matching-based principal component analysis approach. *Knowl.-Based Syst.* **2022**, *250*, 109085. [CrossRef]
31. Mayet, A.M.; Alizadeh, S.M.; Kakarash, Z.A.; Al-Qahtani, A.A.; Alanazi, A.K.; Alhashimi, H.H.; Eftekhari-Zadeh, E.; Nazemi, E. Introducing a Precise System for Determining Volume Percentages Independent of Scale Thickness and Type of Flow Regime. *Mathematics* **2022**, *23*, 1770. [CrossRef]
32. Paniri, M.; Dowlatshahi, M.B.; Nezamabadi-Pour, H. MLACO: A multi-label feature selection algorithm based on ant colony optimization. *Knowl.-Based Syst.* **2019**, *192*, 105285. [CrossRef]
33. Roshani, M.; Phan, G.T.; Ali, P.J.M.; Roshani, G.H.; Hanus, R.; Duong, T.; Corniani, E.; Nazemi, E.; Kalmoun, E.M. Evaluation of flow pattern recognition and void fraction measurement in two phase flow independent of oil pipeline's scale layer thickness. *Alex. Eng. J.* **2021**, *60*, 1955–1966. [CrossRef]
34. Hashemi, A.; Joodaki, M.; Joodaki, N.Z.; Dowlatshahi, M.B. Ant colony optimization equipped with an ensemble of heuristics through multi-criteria decision making: A case study in ensemble feature selection. *Appl. Soft Comput.* **2022**, *124*, 109046. [CrossRef]
35. Roshani, M.; Phan, G.; Roshani, G.H.; Hanus, R.; Nazemi, B.; Corniani, E.; Nazemi, E. Combination of X-ray tube and GMDH neural network as a nondestructive and potential technique for measuring characteristics of gas-oil–water three phase flows. *Measurement* **2021**, *168*, 108427. [CrossRef]
36. Paniri, M.; Dowlatshahi, M.B.; Nezamabadi-pour, H. Ant-TD: Ant colony optimization plus temporal difference reinforcement learning for multi-label feature selection. *Swarm Evol. Comput.* **2021**, *64*, 100892. [CrossRef]
37. Roshani, M.; Phan, G.; Faraj, R.H.; Phan, N.-H.; Roshani, G.H.; Nazemi, B.; Corniani, E.; Nazemi, E. Proposing a gamma radiation based intelligent system for simultaneous analyzing and detecting type and amount of petroleum by-products. *Nucl. Eng. Technol.* **2020**, *53*, 1277–1283. [CrossRef]
38. Dowlatshahi, M.B.; Derhami, V.; Nezamabadi-Pour, H. Fuzzy particle swarm optimization with nearest-better neighborhood for multimodal optimization. *Iran. J. Fuzzy Syst.* **2020**, *17*, 7–24.
39. Lalbakhsh, A.; Afzal, M.U.; Esselle, K. Simulation-driven particle swarm optimization of spatial phase shifters. In Proceedings of the 18th IEEE international Conference on Electromagnetics in Advanced Applications (ICEAA), Cairns, QLD, Australia, 19–23 September 2016; pp. 428–430.
40. Jamshidi, M.; Lalbakhsh, A.; Lotfi, S.; Siahkamari, H.; Mohamadzade, B.; Jalilian, J. A neuro-based approach to designing a Wilkinsonpower divider. *Int. J. RF Microw. Comput.-Aided Eng.* **2020**, *30*, e22091. [CrossRef]

41. Cheng, K.M.; Ip, W. A Novel Power Divider Design with Enhanced Spurious Suppression and Simple Structure. *IEEE Trans. Microw. Theory Tech.* **2010**, *58*, 3903–3908. [CrossRef]
42. Lin, C.-M.; Su, H.-H.; Chiu, J.-C.; Wang, Y.-H. Wilkinson Power Divider Using Microstrip EBG Cells for the Suppression of Harmonics. *IEEE Microw. Wirel. Compon. Lett.* **2007**, *17*, 700–702. [CrossRef]
43. Woo, D.J.; Lee, T.K. Suppression of Harmonics in Wilkinson Power Divider Using Dual-Band Rejection by Asymmetric DGS. *IEEE Trans. Microw. Theory Tech.* **2005**, *53*, 2139–2144.
44. Zhang, F.; Li, C. Power divider with microstrip electromagnetic band gap element for miniaturization and harmonic rejection. *Electron. Lett.* **2008**, *44*, 422–423. [CrossRef]
45. Yang, J.; Gu, C.; Wu, W. Design of Novel Compact Coupled Microstrip Power Divider with Harmonic Suppression. *IEEE Microw. Wirel. Compon. Lett.* **2008**, *18*, 572–574. [CrossRef]
46. Li, J.-L.; Qu, S.-W.; Xue, Q. Capacitively loaded Wilkinson power divider with size reduction and harmonic suppression. *Microw. Opt. Technol. Lett.* **2007**, *49*, 2737–2739. [CrossRef]
47. Gu, J.-Z.; Yu, X.-J.; Sun, X.-W. A compact harmonic-suppressed Wilkinson power divider using C-SCMRC resonators. *Microw. Opt. Technol. Lett.* **2006**, *48*, 2382–2384. [CrossRef]
48. Karthikeyan, S.S.; Kshetrimayum, R. Compact, harmonic suppressed power divider using open complementary split-ring resonator. *Microw. Opt. Technol. Lett.* **2011**, *53*, 2897–2899. [CrossRef]
49. He, J.; Feng, Z.; Chen, B.; Yang, H.; Xiong, M.Y. Miniaturized microstrip Wilkinson power divider with capacitor loading. *Microw. Opt. Technol. Lett.* **2012**, *54*, 61–63. [CrossRef]
50. Wang, J.; Ni, J.; Guo, Y.X.; Fang, D. Miniaturized microstrip Wilkinson power divider with harmonic suppression. *IEEE Microw. Wirel. Compon. Lett.* **2009**, *19*, 440–442. [CrossRef]
51. Hazeri, A.R. A New Miniaturization and the nth Harmonic Suppression of Wilkinson Power. *IEICE Trans. Electron.* **2011**, *E94.C*, 215–219. [CrossRef]
52. Hayati, M.; Roshani, S.; Roshani, S.; Shama, F. A novel miniaturized Wilkinson power divider with nth harmonic suppression. *J. Electromagn. Waves Appl.* **2013**, *27*, 726–735. [CrossRef]
53. Moradi, E.; Moznebi, A.-R.; Afrooz, K.; Movahhedi, M. Gysel power divider with efficient second and third harmonic suppression using one resistor. *AEU-Int. J. Electron. Commun.* **2018**, *89*, 116–122. [CrossRef]
54. Chao SF &Li, Y.R. Miniature filtering power divider with increased isolation bandwidth. *Electron. Lett.* **2014**, *50*, 608–610.
55. Liu, F.-X.; Wang, Y.; Zhang, X.-Y.; Quan, C.-H.; Lee, J.-C. A Size-Reduced Tri-Band Gysel Power Divider with Ultra-Wideband Harmonics Suppression Performance. *IEEE Access* **2018**, *6*, 34198–34205. [CrossRef]
56. Roshani, S.; Jamshidi, M.B.; Mohebi, F.; Roshni, S. Design and Modeling of a Compact Power Divider with Squared Resonators Using Artificial Intelligence. *Wirel. Pers. Commun.* **2021**, *117*, 2085–2096. [CrossRef]
57. Heydari, M.; Roshani, S. Miniaturized Harmonic Suppressed Wilkinson Power Divider using Lumped Components and Resonators. *Wirel. Pers. Commun.* **2021**, *117*, 1527–1536. [CrossRef]
58. Zhan, W.-L.; Zhao, X.-L. Compact filtering power divider with harmonic suppression. *J. Electromagn. Waves Appl.* **2016**, *31*, 243–249. [CrossRef]
59. Li, J.L.; Wang, H.Z.; Wang, J.P.; Gao, S.S.; Yang, X.S.; Shao, W. Miniaturized Wilkinson power dividers with harmonic suppressions. *Electromagnetics* **2016**, *36*, 157–166. [CrossRef]
60. Mirzavand, R.; Honari, M.M.; Abdipour, A.; Moradi, G. Compact microstrip Wilkinson power dividers with harmonic suppression and arbitrary power division ratios. *IEEE Trans. Microw. Theory Tech.* **2013**, *61*, 61–68. [CrossRef]
61. Hayati, M.; Roshani, S. A novel Wilkinson power divider using open stubs for the suppression of harmonics. *ACES* **2013**, *28*, 501–506.
62. Lotfi, S.; Roshani, S.; Roshani, S.; Gilan, M.S. Wilkinson power divider with band-pass filtering response and harmonics suppression using open and short stubs. *Frequenz* **2020**, *74*, 169–176. [CrossRef]
63. Lotfi, S.; Roshani, S.; Roshni, S. Design of a miniaturized planar microstrip Wilkinson power divider with harmonic cancellation. *Turk. J. Electr. Eng. Comput. Sci.* **2020**, *28*, 3126–3136.
64. Roshani, S.; Roshani, S. Design of a compact LPF and a miniaturized Wilkinson power divider using aperiodic stubs with harmonic suppression for wireless applications. *Wirel. Netw.* **2020**, *26*, 1493–1501. [CrossRef]
65. Jamshidi, M.B.; Roshani, S.; Talla, J.; Roshani, S.; Peroutka, Z. Size reduction and performance improvement of a microstrip Wilkinson power divider using a hybrid design technique. *Sci. Rep.* **2021**, *11*, 7773. [CrossRef]